

EP-DT  
Detector Technologies

**CERN Summer Studentship 2021 Report:**  
**High precision calibration of 3D hall probes for**  
**magnet mapping apparatuses.**

Pritindra Bhowmick  
Magnetic Measurement Team, EP-DT-TP  
BS-MS 4<sup>th</sup> year, Department of Physics, IISER Bhopal  
[pritindra.bhowmick@cern.ch](mailto:pritindra.bhowmick@cern.ch)  
[pritindra18@iiserb.ac.in](mailto:pritindra18@iiserb.ac.in)  
[pritindra2001@gmail.com](mailto:pritindra2001@gmail.com)

Supervisor: Dr Nicola Pacifico, EP-DT-TP  
[Nicola.Pacifico@cern.ch](mailto:Nicola.Pacifico@cern.ch)

3 September 2021

Keywords: Hall probes, Hall effect, 3D calibration, Numerical analysis.

# Contents

<b>1</b>	<b>Introduction</b>	<b>3</b>
<b>2</b>	<b>Theory</b>	<b>3</b>
2.1	Sources of Errors . . . . .	5
<b>3</b>	<b>Mathematical Analysis</b>	<b>5</b>
3.1	3D scan with spherical harmonics . . . . .	5
3.1.1	Mixing of spherical harmonics . . . . .	6
3.2	Treating the non-orthogonality . . . . .	6
3.3	Contribution from Single magnetic field . . . . .	8
3.4	Scaling with magnetic field . . . . .	8
3.4.1	Choice of Orthogonal polynomials . . . . .	8
3.4.2	Decomposition in Legendre polynomials . . . . .	9
3.5	Treating temperature dependence . . . . .	10
3.6	Building up the model . . . . .	10
<b>4</b>	<b>Numerical Analysis</b>	<b>10</b>
4.1	Scanning in constant Magnetic field and Mixing in spherical harmonic. . .	11
4.2	Why n=240? Exploiting symmetries in spherical harmonics . . . . .	12
4.3	Treating the non-orthogonality . . . . .	14
4.4	Temperature dependency . . . . .	15
4.5	Complete 3D scan . . . . .	16
4.5.1	Too many parameters! and its Solution . . . . .	16
4.5.2	Numerical Error in calculating $c_l$ . . . . .	17
4.5.3	Scaling $c_l$ with B: Decomposition of $f_l(B)$ into Legendre polynomials	18
4.5.4	Scaling $c_l$ with B: Using Lagrange interpolation to estimate $f_l(B)$ .	20
4.6	Building the Model . . . . .	20
4.7	Finding the magnetic field . . . . .	21
<b>5</b>	<b>Implementation</b>	<b>22</b>
5.1	Generating the data . . . . .	22
5.2	The module that does it all . . . . .	23
5.2.1	Basic functions . . . . .	24
5.2.2	<code>scan_3D</code> . . . . .	24
5.2.3	<code>FindB</code> . . . . .	24
<b>6</b>	<b>Results</b>	<b>25</b>

# 1 Introduction

The magnetic measurement team, within the CERN Experimental Physics Detector Technologies group, oversees the mapping of the field of experimental magnets for High Energy Physics experiments, both inside and outside CERN.

Several measurement gantries are available for Cartesian and cylindrical mapping of different magnet geometries. The gantries implement a custom-built 3D hall probe card. Such card hosts 3 hall probes glued on the three sides of a glass cube, in orthogonal configuration. Hall probes are chosen, over other kind of magnetic probes, for their ability to measure the extremely high fields found HEP experiments, often in the order of several Tesla.

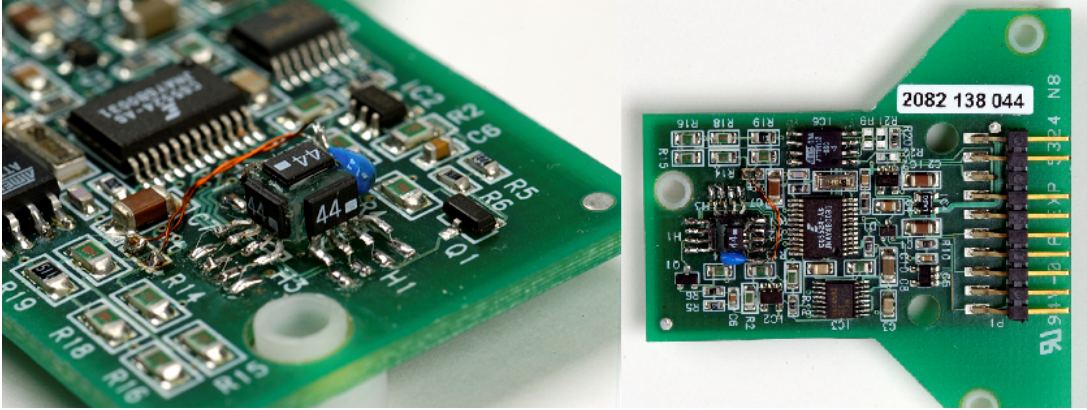


Figure 1: Card with 3 hall probes glued on a glass cube orthogonally.

A precise calibration of the 3 hall probe systems is nevertheless required, to take into account several phenomena that can introduce significant measurement errors. Among them, the relative probe misalignment/non-orthogonality, the hall temperature coefficient, the planar hall effect, various non linearities, etc.

A solution to this problem is the calibration of the 3D system of hall probes by its rotation in a uniform magnetic field, so as to cover the full  $4\pi$  rotation angle and then decompose the hall voltage in solid spherical harmonics.

In this report, we will go through the most important and practical aspects of the process. The objective is to achieve very precise Magnetic field measurements from the hall probes upto the order of  $10^{-4}$  T or lower.

## 2 Theory

If charge conductors with charge  $q$  in a conductors have a mean velocity  $\vec{v}$  and a magnetic field  $\vec{B}$  is applied on the conductor. The charges carriers experience Lorentz force which is given by

$$\vec{F}_l = q\vec{v} \times \vec{B} \quad (1)$$

The current density is given by  $\vec{j} = n'q\vec{v}$  where  $n'$  is the charge carrier concentration. Hence The force experience by a charge carrier is

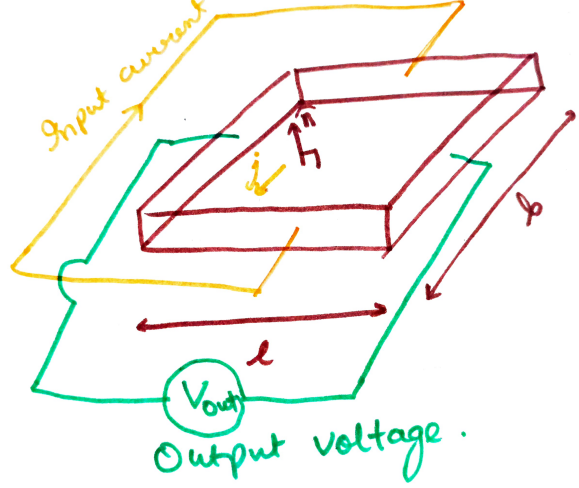
$$\vec{F}_l = \frac{1}{n'} \vec{j} \times \vec{B} \quad (2)$$

Let the normal to Hall probe plane be  $\hat{n}$ . It's obvious that  $\vec{j} \perp \hat{n}$ . The Voltage has a contribution from magnetic field perpendicular to the direction of current  $\vec{j}$  which is given by

$$V_{hall} = RI(\hat{j} \times \vec{B}) \cdot (\hat{j} \times \hat{n}) = RI\hat{n} \cdot \vec{B} \quad (3)$$

Where  $I$  = Hall device Current,  $R = 1/nq$  = Hall coefficient.

The planar hall effect voltage is the contribution to the voltage from the magnetic field in the plane of the hall probe. It is an indication of distortion of lines of current flow produced by the magnetic field. It is given by



$$V_{phe} = G(\vec{B} \times \vec{I})^2 (\vec{B} \cdot \vec{I}) \frac{(\vec{B} \times \vec{I}) \times \vec{I}}{((\vec{B} \times \vec{I}) \times \vec{I})^2} \cdot (\hat{j} \times \hat{n}) \quad (4)$$

$$V_{phe} = GI(\hat{j} \cdot \vec{B})(\hat{n} \cdot (\hat{j} \times \vec{B})) \quad (5)$$

Where  $G$  = Planar hall coefficient.

There is non-linearity due there is a saturation of voltage at very high magnetic fields. Since at CERN, we have very strong magnets, we have to account for the saturation effect. But, the non-linearity can be decreased by decreasing the hall current. We can model it using an infinite series that saturates.

The series expansion of the function can be

$$V_{hall} = RI\hat{n} \cdot \vec{B} + a_1(I\hat{n} \cdot \vec{B})^3 + a_2(I\hat{n} \cdot \vec{B})^5 + \dots \quad (6)$$

Since, the hall effect is odd about the  $\hat{n}$ , only odd terms are there in the series.

For our simulated data, we are using the hyperbolic tangent ( $\tanh(x)$ ) function which can be implemented using a parameter  $\tau$

$$V_{hall} = 2\tau \frac{1 - e^{-RI\hat{n} \cdot \vec{B}/\tau}}{1 + e^{-RI\hat{n} \cdot \vec{B}/\tau}} = 2\tau \tanh \frac{RI\hat{n} \cdot \vec{B}}{2\tau} \quad (7)$$

There can also be possible electronic noise in the system. Let  $\eta$  be the white noise. This gives the output voltage

$$V_{output}(\vec{n}, \vec{j}, \vec{B}) = V_{hall}(\vec{n}, \vec{j}, \vec{B}) + V_{phe}(\vec{n}, \vec{j}, \vec{B}) + \eta \quad (8)$$

The hall coefficient is also dependent on temperature.

## 2.1 Sources of Errors

As discussed above, hall effect is not completely linear. There are a lot of physics contributions that can cause error.

1. Non-linearity
2. Planar Hall Effect (PHE)
3. Non-orthogonality : It is the relative misalignment of the hall probes on the glass cube during gluing.
4. Temperature dependence of hall effect
5. Electronic noise

We have to take into consideration these factors and remove them analytically and numerically. The methods are discussed in subsequent sections.

## 3 Mathematical Analysis

In this section, we will go through the mathematical analysis we went through to get the coefficients. The various methods we used and the challenges faced.

### 3.1 3D scan with spherical harmonics

For a particular magnitude of magnetic field, the output voltage  $V(\vec{B})$  depends only on the polar angle  $\phi$  and azimuthal angle  $\theta$ . We can think of this function on a spherical surface. Such a function can be reduced to spherical harmonic coefficients  $c_{lm}$ .

$$V_{out}(\theta, \phi) = \sum_{l=0}^{\infty} \sum_{m=-l}^l (-1)^m c_{lm} Y_{lm}(\theta, \phi) \quad (9)$$

where

$$c_{lm} = \int d\Omega Y_{l,-m}(\theta, \phi) V_{out}(\theta, \phi) \quad (10)$$

#### Spherical Harmonics

Spherical harmonics are special functions defined on the surface of sphere. They form a complete orthonormal basis for the vector space of functions defined on the surface of the sphere.

$$\int d\Omega Y_{l,m}(\theta, \phi) Y_{l',m'}^*(\theta, \phi) = \delta_{l,l'} \delta_{m,m'} \quad (11)$$

Let  $f(\theta, \phi)$  be any such function, then there exist unique coefficients  $c_{l,m}$  such that

$$f(\theta, \phi) = \sum_{l=0}^{\infty} \sum_{m=-l}^l c_{lm} Y_{lm}(\theta, \phi) \quad (12)$$

A complete list of spherical harmonic functions can be found [here](#).

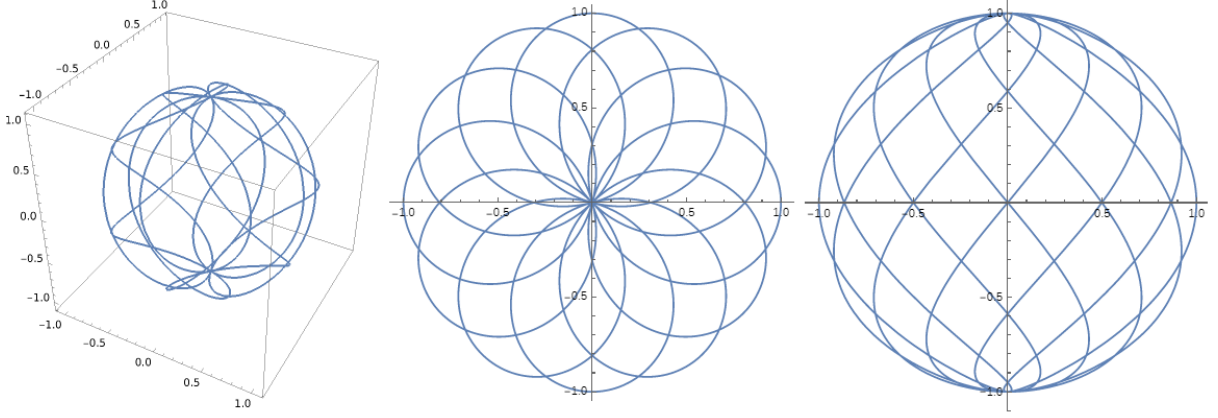


Figure 2: 3D view, side view and top view of the parametrisation

It is not possible to scan the complete surface, so we employ a technique of line integral with 6 turns in outer circle and 5 turns in inner circle as described in figure 2.

The parameterisation is given by

$$\theta(t) = 6t, \phi(t) = 5t + \frac{\pi}{12}, \text{ where } t \in [0, 2\pi] \quad (13)$$

This gives a normalisation factor of  $\pi$ . So, the surface integral becomes

$$c_{lm} = \int_0^{2\pi} dt Y_{l,-m}(6t, 5t) V_{out}(6t, 5t) |\sin(6t)| \pi \quad (14)$$

This gives rise to a different problem.

### 3.1.1 Mixing of spherical harmonics

We know the the spherical harmonics should be perfectly orthogonal i.e.

$$\int d\Omega Y_{l,-m}(\theta, \phi) Y_{l',m'}(\theta, \phi) = (-1)^m \delta_{l,l'} \delta_{m,m'} \quad (15)$$

but,

$$\int_0^{2\pi} dt Y_{5,5}(6t, 5t) Y_{7,7}(6t, 5t) |\sin(6t)| \pi \neq 0 \quad (16)$$

We will discuss the methods of solving this problem in the later sections.

## 3.2 Treating the non-orthogonality

Non-orthogonality is the relative misalignment of the hall probes on the glass cubes. Although the precision of gluing the hall probes is very high ( $\pm 0.01$ ), see [this](#), we still have to figure out the non-orthogonality.

We know the spherical harmonics for  $\ell = 1$  and  $\ell = 2$ . They are

$$Y_1^0(\theta, \varphi) = \frac{1}{2} \sqrt{\frac{3}{\pi}} \cos \theta = \frac{1}{2} \sqrt{\frac{3}{\pi}} \frac{z}{r} \quad (17)$$

$$Y_1^{\pm 1}(\theta, \varphi) = -\frac{1}{2} \sqrt{\frac{3}{2\pi}} e^{\pm i\varphi} \sin \theta = -\frac{1}{2} \sqrt{\frac{3}{2\pi}} \frac{(x \pm iy)}{r} \quad (18)$$

$$Y_2^0(\theta, \varphi) = \frac{1}{4} \sqrt{\frac{5}{\pi}} (3 \cos^2 \theta - 1) = \frac{1}{4} \sqrt{\frac{5}{\pi}} \frac{(3z^2 - r^2)}{r^2} \quad (19)$$

$$Y_2^{\pm 1}(\theta, \varphi) = \frac{1}{2} \sqrt{\frac{15}{2\pi}} e^{\pm i\varphi} \sin \theta \cos \theta = \frac{1}{2} \sqrt{\frac{15}{2\pi}} \frac{(x \pm iy)z}{r^2} \quad (20)$$

$$Y_2^{\pm 2}(\theta, \varphi) = \frac{1}{4} \sqrt{\frac{15}{2\pi}} e^{\pm 2i\varphi} \sin^2 \theta = \frac{1}{4} \sqrt{\frac{15}{2\pi}} \frac{(x \pm iy)^2}{r^2} \quad (21)$$

So we know that, the contribution from hall coefficient is

$$V_{hall} = n_x B_x + n_y B_y + n_z B_z \quad (22)$$

where

$$\hat{n} = (n_x, n_y, n_z), \hat{j} = (j_x, j_y, j_z), \vec{B} = (B_x, B_y, B_z)$$

Hence,

$$n_x = \frac{c_1^1 + c_1^{-1}}{\sqrt{2}t} \frac{1}{\sqrt{\sum_m |c_1^m|^2}}, n_y = \frac{c_1^1 - c_1^{-1}}{\sqrt{2}} \frac{1}{\sqrt{\sum_m |c_1^m|^2}}, n_z = \frac{c_1^0}{\sqrt{\sum_m |c_1^m|^2}} \quad (23)$$

And the contribution from planar hall coefficient is

$$\begin{aligned} V_{phe} = & (j_x j_z n_y - j_x j_y n_z) x^2 + (-j_x j_z n_x + j_y j_z n_y + j_x^2 n_z - j_y^2 n_z) xy \\ & + (-j_y j_z n_x y^2 + j_x j_y n_z) y^2 + (j_x j_y n_x - j_x^2 n_y + j_z^2 n_y - j_y j_z n_z) xz \\ & + (j_y^2 n_x - j_z^2 n_x - j_x j_y n_y + j_x j_z n_z) yz + j_y j_z n_x z^2 - j_x j_z n_y z^2 \end{aligned} \quad (24)$$

and  $j_x, j_y, j_z$  are solution to the following set of non-linear equations

$$-j_x j_z n_x + j_y j_z n_y + j_x^2 n_z - j_y^2 n_z = \frac{c_2^2 - c_2^{-2}}{2i} \frac{1}{\sqrt{\sum_m |c_2^m|^2}} \quad (25)$$

$$j_y^2 n_x - j_z^2 n_x - j_x j_y n_y + j_x j_z n_z = \frac{c_2^1 + c_2^{-1}}{2i} \frac{1}{\sqrt{\sum_m |c_2^m|^2}} \quad (26)$$

$$j_x j_y n_x - j_x^2 n_y + j_z^2 n_y - j_y j_z n_z = \frac{c_2^1 - c_2^{-1}}{2} \frac{1}{\sqrt{\sum_m |c_2^m|^2}} \quad (27)$$

We have to solve the above set of 3 equations to find the 3 unknowns.

### 3.3 Contribution from Single magnetic field

For a perfectly orthogonal hall probe, the following components give the following contributions

- $c_{1,0} \rightarrow$  Hall effect
- $c_{2,2}, c_{2,-2} \rightarrow$  Planar Hall effect
- $c_{3,0}, c_{5,0}, c_{7,0}, c_{9,0}, \dots \rightarrow$  Non-Linearity
- Everything else will be zero.

If we have non-orthogonality, we'll have other contributions. But, We can rotate our axis to the direction of hall probe such that All other factors are zero.

### 3.4 Scaling with magnetic field

For scaling the coefficients of  $Y_{l,m}$  with  $|\vec{B}|$ , we have to use solid harmonics instead of spherical harmonics.

#### Solid Harmonics

Solid harmonics are solutions of the Laplace equation in spherical polar coordinates. They are given by

$$R_{l,m}(r, \theta, \phi) = |r|^l Y_{l,m}(\theta, \phi) \quad (28)$$

The spherical harmonics coefficients  $c_{lm}$  scale more or less with  $|\vec{B}|^l$ . So  $c_{lm} \equiv c_{lm}(B)$ . The output voltage can be decomposed as

$$V_{out}(B, \theta, \phi) = \sum_{l=0}^{\infty} \sum_{m=-l}^l (-1)^m c_{lm}(B) B^l Y_{lm}(\theta, \phi) \quad (29)$$

where  $B = |\vec{B}|$ . We can decompose  $c_{l,m}(B)$  in Orthogonal polynomials which form a complete orthogonal basis of all functions defined in symmetric bounded set  $[-B_{max}, B_{max}]$ . We know that we can scale this set to  $[-1, 1]$ . So, a function in domain  $[-1, 1]$  is equivalently good.

#### 3.4.1 Choice of Orthogonal polynomials

For a choice of orthogonal polynomials defined on a bounded interval, we have two choices,

1. Legendre Polynomials
2. Chebyshev Polynomials

We can compare the two polynomials to judge which one would be more suitable for the analysis

- Both have very similar properties. They lie in the interval  $[-1, 1]$ .



- But for calibration, we are using Legendre-Gauss Quadrature method which is biased towards Legendre polynomials.
- Also, Legendre polynomials decay.
- It gives very accurate decomposition of various components to Legendre polynomials

For the above reasons, we choose Legendre polynomials for the analysis.

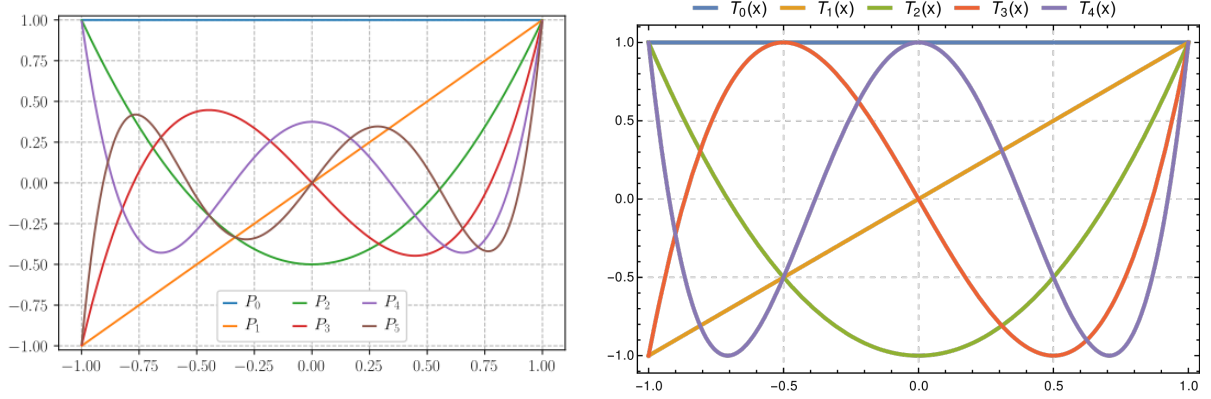


Figure 3: First few Legendre and Chebyshev polynomials.  $P_n$  and  $T_n$  are Legendre and chebyshev polynomials respectively

### 3.4.2 Decomposition in Legendre polynomials

#### Legendre Polynomials

The Legendre differential equation is given by

$$(1 - x^2)y'' - 2xy' + k(k + 1)y = 0 \quad (30)$$

If  $k \in \mathbb{Z}$ , the solutions are a set of orthogonal polynomials  $P_k(x)$  defined in  $[-1, 1]$ . The orthogonality is defined as

$$\int_{-1}^1 dx P_k(x) P_m(x) = \frac{2}{2k + 1} \delta_{k,m} \quad (31)$$

So any function in  $[-1, 1]$  can be decomposed as

$$f(x) = \sum_{k=0}^{\infty} a_k P_k(x) \quad (32)$$

where  $a_k = \frac{2k + 1}{2} \int_{-1}^1 dx P_k(x) f(x)$

We need to find Legendre series coefficients  $a_{lmk}$  such that

$$c_{lm}(B) = B^l \sum_{k=0}^{\infty} a_{lmk} P_l(B/B_{max}) \quad (33)$$

where

$$a_{lmk} = \frac{2k+1}{2} \int_{-1}^1 dB \frac{P_k(B) c_{lm}(B)}{B^l} \quad (34)$$

and  $B_{max}$  = the maximum voltage our sensor reads.

There are some complications with this which we will discuss in numerical analysis. For all cases, the function  $c_{lm}(B)/B^l$  cannot be decomposed into the Legendre polynomials. There, we can use Lagrange interpolation method to calculate  $c_{lm}(B)/B^l$ .

### 3.5 Treating temperature dependence

For small temperature ranges, the temperature dependence on the hall coefficient is linear. So

$$R = R_0 + TR_1 \quad (35)$$

### 3.6 Building up the model

Let  $T_0$  be the temperature the 3D scan was done. We can form the model as

$$V_{model}(\vec{B}, \hat{n}, \hat{j}, T) = \frac{R_0 + TR_1}{R_0 + T_0 R_1} \sum_{l=0}^l \sum_{m=-l}^l \sum_{k=0}^n a_{lmk} B^l P_k(B/B_{max}) Y_{lm}(\theta, \phi) \quad (36)$$

Here  $\theta$  and  $\phi$  are defined as

$$B = |\vec{B}|, \theta = \cos^{-1} \left( \frac{B_z}{B} \right), \phi = \tan^{-1} \left( \frac{B_y}{B_z} \right) \quad (37)$$

If we have 3 hall probes that are more or less orthogonal to each other. And  $V_{model,1}$ ,  $V_{model,2}$ ,  $V_{model,3}$  are the 3 models for the 3 orthogonal probes respectively. If they are giving output voltages  $V_1, V_2, V_3$ , we have to solve the following set of 3 non-linear equations to find the 3 components of magnetic field.

$$V_{model,1}(\vec{B}, \hat{n}_1, \hat{j}_1, T) = V_1 \quad (38)$$

$$V_{model,2}(\vec{B}, \hat{n}_2, \hat{j}_2, T) = V_2 \quad (39)$$

$$V_{model,3}(\vec{B}, \hat{n}_3, \hat{j}_3, T) = V_3 \quad (40)$$

Solving these equations gives the required voltage.

## 4 Numerical Analysis

In the previous section, we discussed the mathematics behind the calibration. We have employed various techniques of Numerical integration, Numerical solvers, Curve fitters,

Interpolation techniques and many more to arrive to precise numbers. In this section, we shall discuss the numerical analysis behind it, why a particular method was chosen over another, what kind of accuracy and errors they gave and what methods were further used to rectify those errors.

#### 4.1 Scanning in constant Magnetic field and Mixing in spherical harmonic.

Let us define a particular notation which will help us to understand the problem.

$$|l, m\rangle = Y_{l,m}(\theta, \phi) \quad (41)$$

$$\langle l, m| = Y_{l,m}^*(\theta, \phi) \quad (42)$$

$$\langle l, m|l', m'\rangle = \int_0^{2\pi} dt Y_{l,-m}(6t, 5t) Y_{l',m'}(6t, 5t) |\sin(6t)|\pi \quad (43)$$

We conduct this integration by the Simpson 1/3 rule.

$$\langle l, m|l', m'\rangle = \frac{2\pi}{3n} \left( g(x_0) + 4 \sum_{i=odd} g(x_i) + 2 \sum_{j=even} g(x_j) + g(x_n) \right) \quad (44)$$

where  $g(x) = Y_{l,-m}(6t, 5t) Y_{l',m'}(6t, 5t) |\sin(6t)|\pi$  and  $x_i = 2\pi i/n$ .

##### Simpson's 1/3 method

Simpson's 1/3 rule results when a second-order interpolating polynomial is substituted into the quadrature formula. For 3 points, the formulae is given by

$$\int_{x_0}^{x_0+2h} f(x)dx = \frac{h}{3} (f(x_0) + 4f(x_1) + f(x_2)) \quad (45)$$

where  $x_i = x_0 + ih$ . For  $n + 1$  equidistant points, it is given by

$$\int_a^b f(x)dx = \frac{h}{3} \left( f(x_0) + 4 \sum_{i=odd} f(x_i) + 2 \sum_{j=even} f(x_j) + f(x_n) \right) \quad (46)$$

Here  $h = (b-a)/n$  and  $x_i = x_0 + ih$ . The approximate error is  $(b-a)^5 f^{(4)}(\xi)/180n^4$ . For more details, one can visit the [wikipedia page](#).

We take **n=240 points** around the spherical surface as described in the figure. This gives rise to some mixing due to parametrisation bias and numerical error. i.e,

$$\langle l, m|l', m'\rangle \neq \delta_{ll'} \delta_{mm'} \quad (47)$$

Let the required function to be decomposed is  $|V\rangle = V(\theta, \phi)$ .

$$V(\theta, \phi) = \sum_{l=0}^{l_{max}} \sum_{m=-l}^l c_{lm} |l, m\rangle \quad (48)$$

If we take an inner product with  $|l', m'\rangle$ , we get

$$c'_{l,m} = \langle l', m' | V \rangle = \sum_{l=0}^{l_{max}} \sum_{m=-l}^l c_{lm} \langle l', m' | l, m \rangle \quad (49)$$

If we define a matrix such that

$$M = \begin{pmatrix} \langle 0, 0 | 0, 0 \rangle & \langle 0, 0 | 1, -1 \rangle & \langle 0, 0 | 1, 0 \rangle & \langle 0, 0 | 1, 1 \rangle & \dots \\ \langle 1, -1 | 0, 0 \rangle & \langle 1, -1 | 1, -1 \rangle & \langle 1, -1 | 1, 0 \rangle & \langle 1, -1 | 1, 1 \rangle & \dots \\ \langle 1, 0 | 0, 0 \rangle & \langle 1, 0 | 1, -1 \rangle & \langle 1, 0 | 1, 0 \rangle & \langle 1, 0 | 1, 1 \rangle & \dots \\ \langle 1, 1 | 0, 0 \rangle & \langle 1, 1 | 1, -1 \rangle & \langle 1, 1 | 1, 0 \rangle & \langle 1, 1 | 1, 1 \rangle & \dots \\ \dots & \dots & \dots & \dots & \dots \end{pmatrix} \quad (50)$$

and vectors

$$C' = (c'_{0,0}, c'_{1,-1}, c'_{1,0}, c'_{1,-1}, \dots) \quad (51)$$

and

$$C = (c_{0,0}, c_{1,-1}, c_{1,0}, c_{1,-1}, \dots) \quad (52)$$

So, we get

$$C' = CM \quad (53)$$

$$\implies C = C' M^{-1} \quad (54)$$

This method works because in principal, the spherical harmonic are orthonormal set of functions. still, for  $l_{max} > 10$ , the matrix M is singular. But  $l_{max} = 10$  provides good enough accuracy and capture good amount of physics.

## 4.2 Why n=240? Exploiting symmetries in spherical harmonics

The higher the number of points, the accurate the numerical integral is. But some points give greater accuracy than others.

For examples: Consider numerically integrating an odd function  $f_o(x)$  in the domain  $[-a, a]$ . If we take equidistant points given by  $x_i = -a + ai/n$  for  $0 \leq i \leq 2n$ , We get  $f_o(x_i) = -f_o(x_{2n-i})$

$$I = \int_{-a}^a f_o(x) dx = 0 \quad (55)$$

But if we take  $x_i = -a + ai/n + a/3n$ , we get no such cancellation and  $I$  may or may not be zero depending on the properties of  $f_o(x)$ .

$n = 240$  is one such sweet spot. We know that increasing the number of points increases the complexity and load on machine, but it also gives a more accurate answer. So its a trade off.

Carefully looking at Figure 4, we see that for  $Y_{1,1}$ ,  $n = 30$  gives a good cancellation between points. Let  $Y_{1,1}(t) = Y_{1,1}(\theta(t), \phi(t))$ , then  $Y_{1,1}(t) = -Y_{1,1}(t + \pi)$ . That is because

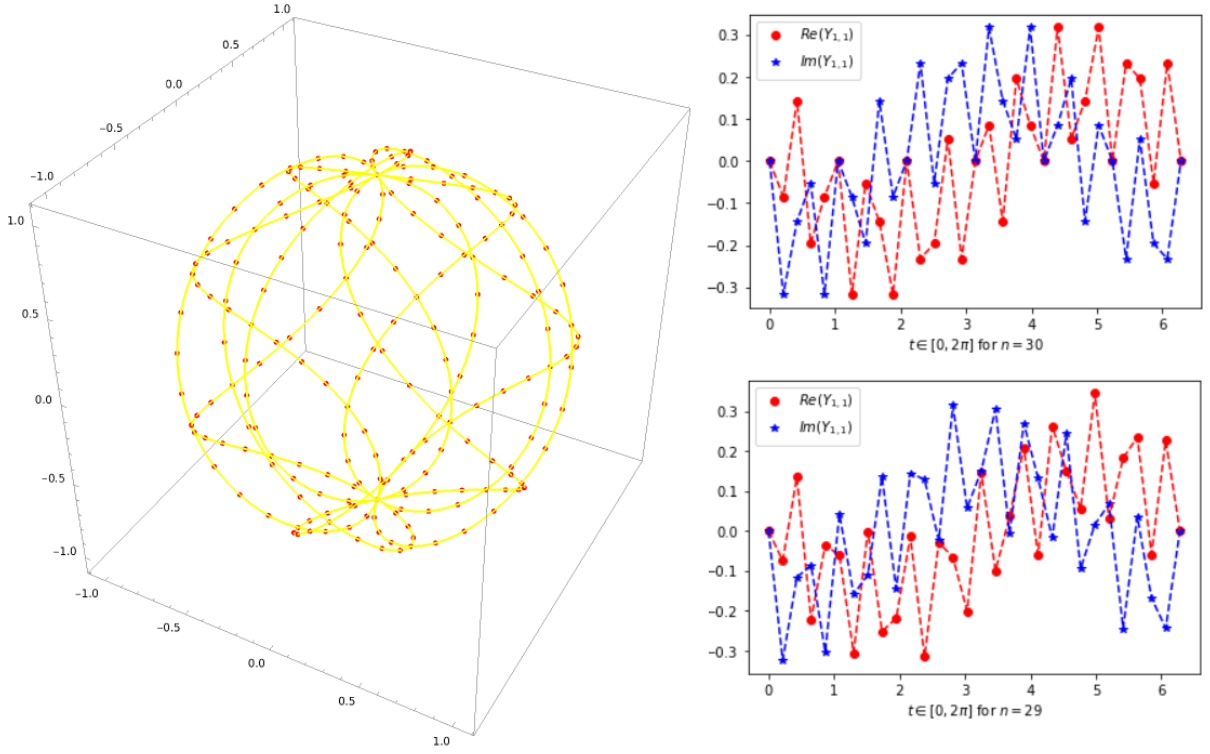


Figure 4:  $n = 240$  points on the surface of sphere, Value of  $Y_{1,1}$  for  $n = 30$  and  $n = 29$

$n = 30 = 5 \times 6$  and we have a parametrisation of  $\theta = 5t$  and  $\phi = 5t + \pi/12$ . But there is no cancellation if  $n = 29$ . So  $n$  has to be a multiple of 30.

Now consider the integral

$$\int_0^{2\pi} dt Y_{1,1}(\theta, \phi) Y_{2,-1}(\theta, \phi) |\sin(\theta)| \quad (56)$$

From Figure 5, if we take  $n = 30$ , there is no cancellation. But if we take  $n = 120$ , there is a clear cancellation and we get a perfect zero. So  $n$  has to be a multiple of 120.

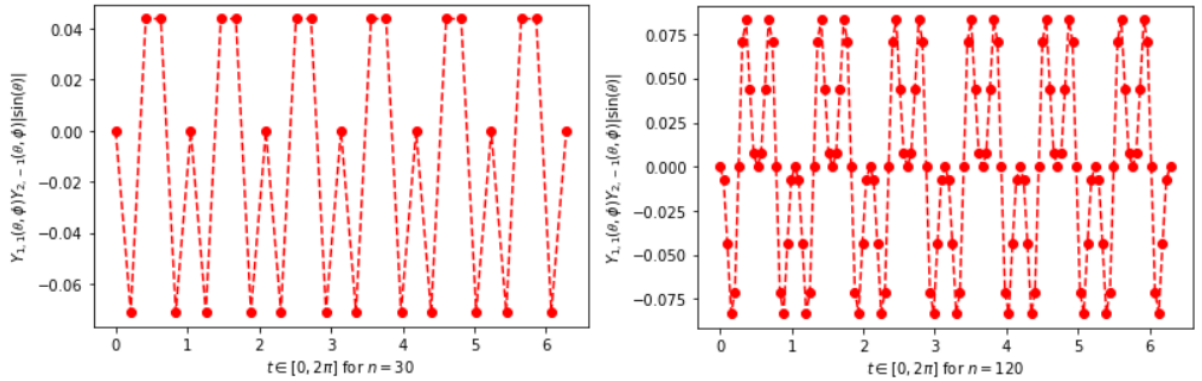


Figure 5:  $Y_{1,1}(\theta, \phi) Y_{2,-1}(\theta, \phi) \sin \theta$  for  $n = 30$  and  $n = 120$ .

But for some other integrals like

$$\int_0^{2\pi} dt Y_{3,1}(\theta, \phi) Y_{1,-1}(\theta, \phi) |\sin(\theta)| \quad (57)$$

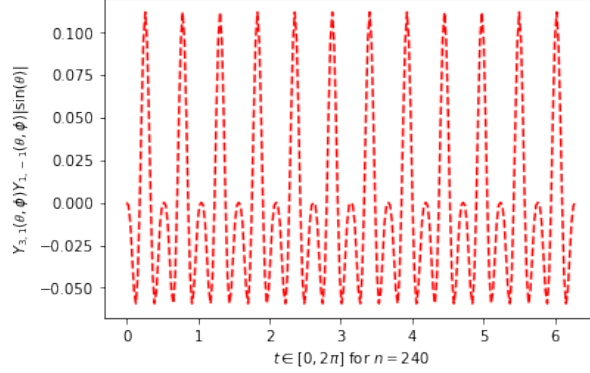
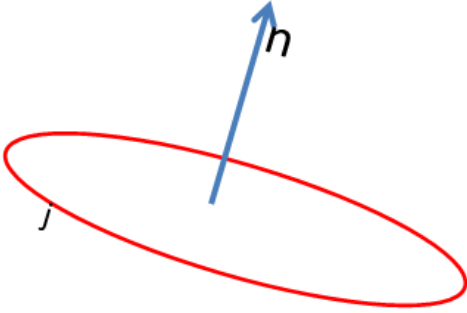


Figure 6:  $Y_{3,1}(\theta, \phi) Y_{1,-1}(\theta, \phi) \sin \theta$  for  $n = 1200$ .

there is no cancellation for any  $n$  even if the value of integral is zero (Figure 6). There is numerical error which is inversely proportional to number of points.  $\mathbf{n}=240$  gives the perfect balance between complexity and accuracy. Numerical error can be fixed by the above method of taking an inverse of matrix and fixing  $\langle l, m | l', m' \rangle \neq \delta_{ll'} \delta_{mm'}$ . For a greater accuracy, one can take  $n = 360$ .

### 4.3 Treating the non-orthogonality



As discussed in section ??, calculating the normal is very straightforward. Main difficulty comes in calculating the direction of current  $\hat{j}$ . But we know that  $\hat{j} \perp \hat{n}$  and its a unit vector. So, it lies on a circle, as shown in figure, which has only one parameter. We know that on this circle, there are two possible solutions to these equations,  $(j_x, j_y, j_z)$  and  $-(j_x, j_y, j_z)$ . Finding any one of them is sufficient.  $j_x, j_y, j_z$  are satisfy following set of non-linear equations

$$f_1(\psi) = j_y j_z n_y - j_x j_z n_x + j_x^2 n_z - j_y^2 n_z - \frac{c_2^2 - c_2^{-2}}{2i} \frac{1}{\sqrt{\sum_m |c_2^m|^2}} = 0 \quad (58)$$

$$f_2(\psi) = j_y^2 n_x - j_z^2 n_x - j_x j_y n_y + j_x j_z n_z - \frac{c_2^1 + c_2^{-1}}{2i} \frac{1}{\sqrt{\sum_m |c_2^m|^2}} = 0 \quad (59)$$

$$f_3(\psi) = j_x j_y n_x - j_x^2 n_y + j_z^2 n_y - j_y j_z n_z - \frac{c_2^1 - c_2^{-1}}{2} \frac{1}{\sqrt{\sum_m |c_2^m|^2}} = 0 \quad (60)$$

So there is a solution in  $[0, \pi]$  of this parametrisation. We divide this interval into two parts:  $[0, \pi/2]$  and  $[\pi/2, \pi]$  and use bisection algorithm to find the solution in both these intervals, the solution has to be in one of them.

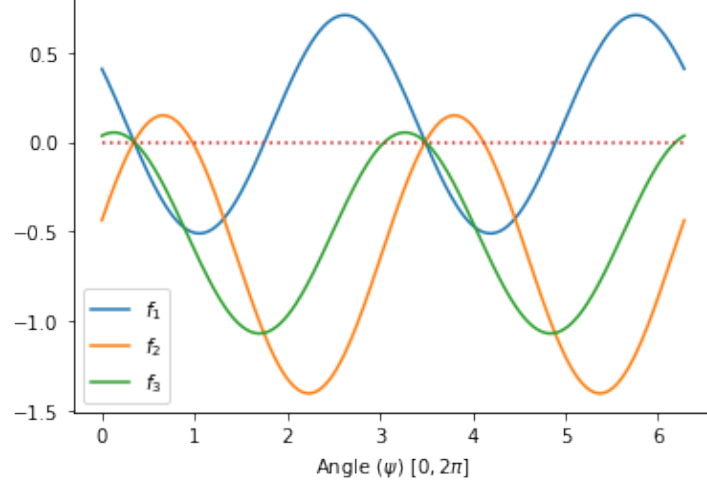


Figure 7: The values of  $f_1, f_2, f_3$  on the circle for a random  $\hat{n}$  and  $\hat{j}$

#### Bisection method

Bisection method is a bracketing method of finding roots of a function in one dimensional function. Let the function be  $f(x)$  defined on some interval where we have to find its root. It involves the following steps.

1. We take an interval  $[x_l, x_u]$ . If  $f(x_l)f(x_u) < 0$ , there lies a root in the interval.
2. We choose  $x_m = (x_l + x_u)/2$ . If  $f(x_l)f(x_m) = 0$ , then  $x_m$  is the solution, end process. If  $f(x_l)f(x_m) < 0$ , then  $x_u = x_m$ . Else if,  $f(x_u)f(x_m) < 0$ , then  $x_l = x_m$ .
3. We repeat the above process until we get the required level of accuracy.

This process is slowly converging but can provide any requirement of accuracy.

## 4.4 Temperature dependency

As stated in section 3.5, we will do a linear fit for the temperature dependence. We take two temperatures  $T_0 = 20^\circ\text{C}$  and  $T_1 = 25^\circ\text{C}$ . We choose to take reading at the highest magnetic field to get two hall coefficient given by

$$R(T)IB = \sqrt{\frac{3}{4\pi}} (|c_{1,0}|^2 + |c_{1,1}|^2 + |c_{1,-1}|^2)^{1/2} \quad (61)$$

$$R(T) = \sqrt{\frac{3}{4\pi}} \frac{(|c_{1,0}|^2 + |c_{1,1}|^2 + |c_{1,-1}|^2)^{1/2}}{IB} = \sqrt{\frac{3}{4\pi}} \frac{c_1}{IB} \quad (62)$$

Here  $I$  = hall current and  $B = |\vec{B}|$ . From linear fit, we get

$$R = R_0 + TR_1 \quad (63)$$

where

$$R_1 = \frac{R(25) - R(20)}{25 - 20} = \frac{R(25) - R(20)}{5} \quad (64)$$

$$R_0 = \frac{1}{2}(R(25) + R(20) - R_1(20 + 25)) = \frac{1}{2}(R(25) + R(20) - 45R_1) \quad (65)$$

Taking more than 2 points will increase the accuracy of the fit.

### Linear Regression

The simplest form of regression analysis, linear regression is used in fitting a straight line to a set of paired observations:  $(x_1, y_1), (x_2, y_2), \dots, (x_n, y_n)$ . Not going too deep into the least square error, the intercept and slope of the graph are given by

$$m = \frac{n \sum x_i y_i - \sum x_i \sum y_i}{n \sum x_i^2 - (\sum x_i)^2} \quad (66)$$

$$c = \frac{1}{n} \left( \sum y_i - m \sum x_i \right) \quad (67)$$

We can check the error by the Pearson correlation coefficient given by

$$R = \frac{n \sum x_i y_i - \sum x_i \sum y_i}{\sqrt{n \sum x_i^2 - (\sum x_i)^2} \sqrt{n \sum y_i^2 - (\sum y_i)^2}} \quad (68)$$

If  $|R| \approx 1$ , then it's a good fit. More details can be found [here](#).

## 4.5 Complete 3D scan

We are going to discuss the most important part of our analysis. We discussed the mathematics behind 3D scan in sections 3.1 and 3.4. In this section we discuss how we conducted the complete 3D scan and the numerical methods used.

### 4.5.1 Too many parameters! and its Solution

There is a problem with the method if we continue conventionally.

1. If we calibrate for  $l \leq 10$ , we will have 100 constants.
2. That means 100  $c_{l,m}(B)$  functions.
3. If we take 10 Legendre series coefficients, It will be about 1000 constants.
4. This will make our model impossible to build and Our calibration very difficult.
5. Reverting the equation will also be impossible.



To solve that, we have to take into account the non-orthogonality of the hall probes.

In section 3.3, we discussed how rotating our axis in the direction of  $\hat{n}$  and  $\hat{j}$  can solve the extra contributions we get from non-orthogonality. We also obtained the values of  $c_{l,m}$  in section 4.1. One of the most important things to understand here is :

For rotation of axis,  $c_l^2 = \sum_{m=-l}^l |c_{l,m}|^2$  remains constant.

Now, the ratio of  $c_{l,m}$  for all  $m$  remain same for a particular value of  $l$  even if we increase the magnitude of magnetic field. Mathematically, for a fixed  $l$ ,

$$\vec{r}_l \equiv \frac{(c_{l,-m}, c_{l,-m+1}, c_{l,-m+2}, \dots, c_{l,m-1}, c_{l,m})}{\sqrt{\sum_{m=-l}^l |c_{l,m}|^2}} = \text{constant for all } |\vec{B}| \quad (69)$$

Then we get

$$c_{l,m} = r_l[m] \times c_l \quad (70)$$

Obtaining  $r_l$  is too easy if we know  $c_{lm}$ !

So, for 3D scan, we can find how  $c_l$  scales with  $B = |\vec{B}|$  and then using the vector  $\vec{r}_l$ , we can decompose the scaling into different  $c_{l,m}$ . This solves our too many parameters problem.

Let us define a function which will be used in rest of the literature

$$f_l(B) = c_l(B)/B^l \quad (71)$$

#### 4.5.2 Numerical Error in calculating $c_l$

For small magnetic field, the contribution from higher order term  $l \geq 5$  is very small and has numerical errors, but for high magnetic field, it is quite accurate. Reason being, `numpy float` has a maximum precision of  $10^{-16}$ . This leads to numerical errors. Usually contributions of order  $c_l \sim 10^{-10}$  are ignored. But this will affect decomposition of  $c_l$  into Legendre polynomials.

So, there are some points which are ignored (for small  $B$ ) and the points remain for larger values of  $B$ . We evaluate the missing points using Lagrange interpolation. If the interpolation function is  $\mathbb{L}_l(B) \equiv f_l(B)$ , then we assign

$$c_l(B_j) = \mathbb{L}_l(B_j)B_j^l \quad (72)$$

where  $B_j$  are the points that were ignored. We know that the function  $f_l(B)$  is even. So we use a special case of Lagrange interpolation for even functions.

To explain by example, In the figure 8 of  $f_9 = c_9(B)/B^9$ , one can observe that without interpolation, there is an error for  $c_9(B)/B^9$  for the lowest  $B$ . So we remove it, conduct a Lagrange interpolation on rest of the points and evaluate  $c_9(B)/B^9$  for the lowest value. This is quite accurate and gives correct results.

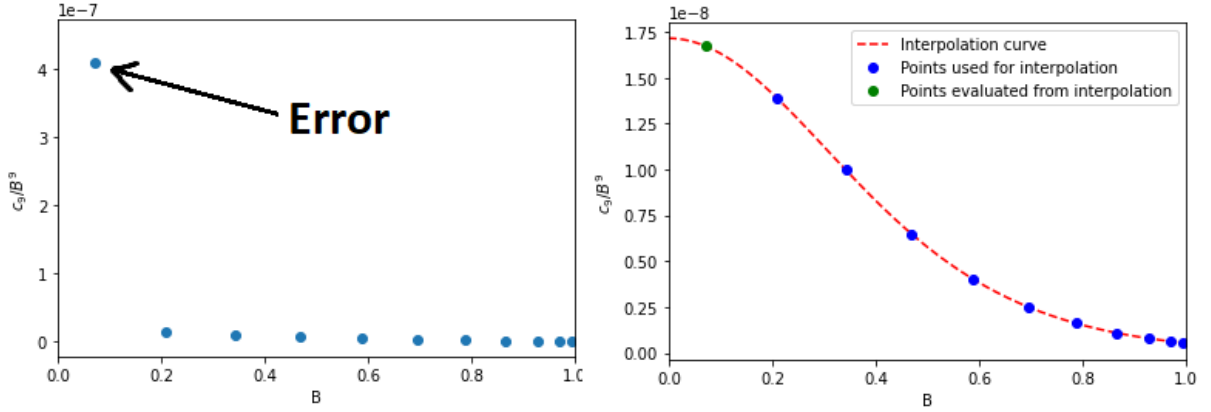


Figure 8: Original evaluation of  $c_9(B)/B^9$  with error and Lagrange interpolation results.

### Lagrange interpolation

Lagrange interpolation is a polynomial interpolation such that for a given set of points  $(x_j, y_j)$  with no two  $x_j$  values equal, the Lagrange interpolation gives a polynomial of lowest degree that takes at each value  $x_j$  the corresponding value  $y_j$ , so that the functions coincide at each point.

Given a set of  $n + 1$  data points  $(x_0, y_0), \dots, (x_j, y_j), \dots, (x_n, y_n)$ , the interpolation polynomial in the Lagrange form is given by

$$\mathbb{L}(x) := \sum_{j=0}^n y_j \ell_j(x) \quad (73)$$

where

$$\ell_j(x) := \prod_{\substack{0 \leq m \leq n \\ m \neq j}} \frac{x - x_m}{x_j - x_m} = \frac{(x - x_0)}{(x_j - x_0)} \dots \frac{(x - x_{j-1})}{(x_j - x_{j-1})} \frac{(x - x_{j+1})}{(x_j - x_{j+1})} \dots \frac{(x - x_n)}{(x_j - x_n)} \quad (74)$$

For even function, we know that only the even powers of  $x$  exist and odd power terms are zero. Using the philosophy of Lagrange interpolation, We take

$$\ell_j(x) := \prod_{\substack{0 \leq m \leq n \\ m \neq j}} \frac{x^2 - x_m^2}{x_j^2 - x_m^2} = \frac{(x^2 - x_0^2)}{(x_j^2 - x_0^2)} \dots \frac{(x^2 - x_{j-1}^2)}{(x_j^2 - x_{j-1}^2)} \frac{(x^2 - x_{j+1}^2)}{(x_j^2 - x_{j+1}^2)} \dots \frac{(x^2 - x_n^2)}{(x_j^2 - x_n^2)} \quad (75)$$

#### 4.5.3 Scaling $c_l$ with B: Decomposition of $f_l(B)$ into Legendre polynomials

**type1 == 'B':** This method works only if we have the liberty to choose the magnitude of magnetic fields scanning is done.

From section 3.4, we have the idea of that  $c_l \propto B^l$  and for more accuracy, we will

decompose  $f_l(B)$  into Legendre polynomials. Suppose the maximum limit of magnetic field we want our system to measure is  $B_{max}$ . Then, We need to find Legendre series coefficients  $a_{lk}$  such that

$$f_l(B) = \sum_{k=0} a_{lk} P_k(B/B_{max}) \quad (76)$$

$$\Rightarrow c_l(B) = B^l \sum_{k=0} a_{lk} P_k(B/B_{max}) \quad (77)$$

$$\text{where } a_{lk} = \frac{2k+1}{2} \int_{-1}^1 dB \frac{P_k(B/B_{max}) c_l(B)}{B^l} \quad (78)$$

We can implement Legendre-Gauss Quadrature method here to find calculate the integrals.

#### Legendre-Gauss quadrature method

A quadrature rule is an approximation of the definite integral of a function, usually stated as a weighted sum of function values at specified points within the domain of integration.

In Legendre-Gauss quadrature method, the principle is to decompose the given function  $f(x)$  into Legendre polynomials up to a highest degree  $n$  (order of Gauss quadrature) and once we know coefficients, we know the integral.

An integral in interval  $[-1, 1]$  is given by

$$\int_{-1}^1 f(x) dx \approx \sum_{i=1}^n w_i f(x_i) \quad (79)$$

here, the  $i$ -th Gauss node,  $x_i$ , is the  $i$ -th root of  $P_n$  and the weights are given by

$$w_i = 2/(1 - x_i^2)[P'_n(x_i)]^2 \quad (80)$$

If we want to integrate a function  $g(x)$  in interval  $[a, b]$ , we can use the following transformation.

$$f(x) = g((b-a)x/2 + (b+a)/2) \quad (81)$$

$$f(-1) = g(a) \text{ and } f(1) = g(b) \quad (82)$$

We want to decompose the function  $f_l(B)$  which is an even function. So it will be decomposed into only the even degree Legendre polynomials and odd terms will be zero. We calculate  $f_l(B)$  only for specific magnitudes of magnetic field. If we don't have the liberty to choose magnetic fields, this method fails. These magnetic fields are given by,

$$B_i = x_i B_{max} \quad (83)$$

such that  $x_i$  is positive. and  $w_i$ 's are even for even order, i.e.  $w_i = w_{ord-i}$ . Here  $ord$  = the order of Gauss quadrature. We purposefully choose  $ord$  to be an even number.

Let  $f_e$  be an even function. Since both the function and the weights are even,  $f_e(x_i)w_i = f_e(x_{ord-i})w_{ord-i}$ , and we can estimate the integral as

$$a_{lk} = \frac{2k+1}{2} \sum_{i=1}^{ord} \frac{P_k(B_i/B_{max})c_l(B_i)w_i}{B_i^l} = (2k+1) \sum_{i=ord/2}^{ord} \frac{P_k(B_i/B_{max})c_l(B_i)w_i}{B_i^l} \quad (84)$$

Here,  $c_l(B)$  is calculated using methods describes in sections 4.1 and ??.

#### 4.5.4 Scaling $c_l$ with B: Using Lagrange interpolation to estimate $f_l(B)$

**type1 == 'A': This method works only if we do not have the liberty to choose the magnitude of magnetic fields scanning is done and we have to work with specific values usually linearly spaced.**

If we don't have the choice in what magnetic fields scanning is done, we can't do Legendre Gauss quadrature integration and Legendre polynomials have higher than usual errors. Instead, we can calculate  $f_l(B)$  using Lagrange interpolation. If the scanning is done on  $B_j = B_1, B_2, B_3, \dots$ , then we define

$$f_{l,j} = f_l(B_j) \quad (85)$$

Then, these values can be used for Lagrange interpolation. Since  $f_l$  is even, we use the even version of interpolation. If  $\mathcal{L}_l(B) \approx f_l(B)$  is the Lagrange interpolation function calculated using data points  $(B_j, f_{l,j})$  for  $j = 1, 2, 3, \dots$ , then

$$c_l(B) = B^l \mathcal{L}_l(B) \quad (86)$$

## 4.6 Building the Model

The scaling of output voltage with magnetic field is given by

$$\text{If type1 == 'A' : } f_l(B) = \mathcal{L}_l(B) \quad (87)$$

$$\text{If type1 == 'B' : } f_l(B) = \sum_{k=0} a_{lk} P_k(B/B_{max}) \quad (88)$$

The angular dependence is given by

$$\sum_{m=-l}^l r_l[m] Y_{lm}(\theta, \phi) \quad (89)$$

Here  $\theta$  and  $\phi$  are defined as

$$B = |\vec{B}|, \theta = \cos^{-1} \left( \frac{B_z}{B} \right), \phi = \tan^{-1} \left( \frac{B_y}{B_z} \right) \quad (90)$$

The temperature dependence can be added from the data from linear fit

$$\frac{R_0 + TR_1}{R_0 + T_0R_1} \quad (91)$$

Combining all this, the model becomes

$$V_{model}(\vec{B}, \hat{n}, \hat{j}, T) = \frac{R_0 + TR_1}{R_0 + T_0R_1} \sum_{l=0} B^l f_l(B) \left( \sum_{m=-l}^l r_l[m] Y_{lm}(\theta, \phi) \right) \quad (92)$$

## 4.7 Finding the magnetic field

Once we have built our model for the 3 hall probes, we have to solve the following 3 non-linear equations in 3 variables.

$$f_1(B_x, B_y, B_z) = V_{model,1}(\vec{B}, \hat{n}_1, \hat{j}_1, T) - V_1 = 0 \quad (93)$$

$$f_2(B_x, B_y, B_z) = V_{model,2}(\vec{B}, \hat{n}_2, \hat{j}_2, T) - V_2 = 0 \quad (94)$$

$$f_3(B_x, B_y, B_z) = V_{model,3}(\vec{B}, \hat{n}_3, \hat{j}_3, T) - V_3 = 0 \quad (95)$$

where  $V_{model,1}$ ,  $V_{model,2}$ ,  $V_{model,3}$  are the 3 models for the 3 orthogonal probes which are giving output voltages  $V_1, V_2, V_3$  respectively. We will solve this using Multidimensional Newton-Raphson method.

### General Multidimensional Newton-Raphson method

This is a method of solving multiple equations such that number of unknowns is same as number of equations. Suppose we have  $n$  equations and unknowns. We have to solve:

$$f(x) = \begin{pmatrix} f_1(x_1, x_2, x_3, \dots, x_n) \\ f_2(x_1, x_2, x_3, \dots, x_n) \\ f_3(x_1, x_2, x_3, \dots, x_n) \\ \dots \\ f_n(x_1, x_2, x_3, \dots, x_n) \end{pmatrix} = 0 \quad (96)$$

where  $x = (x_1, x_2, x_3, \dots, x_n) \in \mathbb{R}^n$  and  $f : \mathbb{R}^n \rightarrow \mathbb{R}^n$ . Given a guess  $x$ , we want to find a better guess, say,  $x + \delta$  for some  $\delta \in \mathbb{R}^n$ . Taylor expanding  $f$  to first order, we get

$$f(x + \delta) = f(x) + J(x)\delta = 0 \quad (97)$$

where  $J(x) = [\partial f_i / \partial x_j]$  is the Jacobian matrix. Hence we get

$$\delta = -J(x)^{-1} f(x) \quad (98)$$

replacing  $x \rightarrow x + \delta$  and repeating the above step to get desired level of accuracy, we can find the solution for the given set of equations. Note that  $J(x)$  has to be invertible for this method to work. For more details see [this](#).

We define function

$$V(B_x, B_y, B_z) = (V_1(B_x, B_y, B_z), V_2(B_x, B_y, B_z), V_3(B_x, B_y, B_z)) \quad (99)$$

We solve the equations in the following steps:

1. We know that the 3 hall probes point in  $\hat{x}, \hat{y}, \hat{z}$  directions. Also, for a given temperature hall coefficient  $R$  is known. If  $i$  is the input current, our initial guess is

$$B_g = (V_1, V_2, V_3)/IR \quad (100)$$

2. We take a step size of  $dB = 0.01$  T and calculate  $J(B)$  by

$$J(B) = \frac{1}{dB} \begin{pmatrix} V(B_x + dB, B_y, B_z) - V(B_x, B_y, B_z) \\ V(B_x, B_y + dB, B_z) - V(B_x, B_y, B_z) \\ V(B_x, B_y, B_z + dB) - V(B_x, B_y, B_z) \end{pmatrix} \quad (101)$$

3. We calculate  $\delta$  by

$$\vec{\delta} = -V(B_x, B_y, B_z) \times J(B) \quad (102)$$

and replace  $\vec{B} \rightarrow \vec{B} + \vec{\delta}$ .

4. Repeat steps 2 and 3 until we reach a desired level of accuracy.

## 5 Implementation

In this section, we will discuss the implementation of the code in a step by step format. For more details, please find the complete code and related files at the github repository [https://github.com/pritindra-bhowmick/Hall\\_Probes\\_3D\\_calibration\\_CERN](https://github.com/pritindra-bhowmick/Hall_Probes_3D_calibration_CERN)

### 5.1 Generating the data

Here we will discuss methods used to generate simulated data.

1. Set up the output voltage of a hall probe using

$$V_{output}(\vec{n}, \vec{j}, \vec{B}, T) = V_{hall}(\vec{n}, \vec{j}, \vec{B}) + V_{phe}(\vec{n}, \vec{j}, \vec{B}) + \eta \quad (103)$$

$$= R(T)I\hat{n}.\vec{B} + GI(\hat{j}.\vec{B})(\hat{n}.\hat{j} \times \vec{B}) + a_1(I\hat{n}.\vec{B})^3 + a_2(I\hat{n}.\vec{B})^5 + \dots + \eta \quad (104)$$

we can define  $R(T), I, G, a_1, a_2, \dots, \eta$  can be defined.

2. The parametrisations were defined earlier. To rotate a vector in that way, we have to use rotation matrix

$$Rot(t) = \begin{pmatrix} \cos \phi(t) \cos \theta(t) & -\sin \phi(t) & \sin \theta \cos \phi(t) \\ \sin \phi(t) \cos \theta(t) & \cos \phi(t) & \sin \theta \sin \phi(t) \\ -\sin \theta(t) & 0 & \cos \theta(t) \end{pmatrix} \quad (105)$$

if  $t \in [0, 2\pi]$ ,  $\vec{B}_0$  is the initial magnetic field and we want to rotate  $\vec{B}_0$  in the parametric way as shown in the figure. We should have

$$\vec{B}(t)^\dagger = Rot(t)\vec{B}_0^\dagger \quad (106)$$

3. Instead, the machine rotates the hall probes, which can be modelled as

$$\hat{n}.\vec{B}(t) = \hat{n}\vec{B}(t)^\dagger = \hat{n}Rot(t)\vec{B}_0^\dagger = \hat{n}(t)\vec{B}_0^\dagger = \hat{n}(t).\vec{B}_0 \quad (107)$$

Similarly  $\hat{j}$  can be modelled as

$$\hat{j}.\vec{B}(t) = \hat{j}\vec{B}(t)^\dagger = \hat{j}Rot(t)\vec{B}_0^\dagger = \hat{j}(t)\vec{B}_0^\dagger = \hat{j}(t).\vec{B}_0 \quad (108)$$

4. Introducing non-orthogonality can be done by multiplying  $\hat{n}$  and  $\hat{j}$  with rotation matrices defined as

$$R_i = \begin{bmatrix} \cos \alpha_i \cos \beta_i & \cos \alpha_i \sin \beta_i \sin \gamma_i - \sin \alpha_i \cos \gamma_i & \cos \alpha_i \sin \beta_i \cos \gamma_i + \sin \alpha_i \sin \gamma_i \\ \sin \alpha_i \cos \beta_i & \sin \alpha_i \sin \beta_i \sin \gamma_i + \cos \alpha_i \cos \gamma_i & \sin \alpha_i \sin \beta_i \cos \gamma_i - \cos \alpha_i \sin \gamma_i \\ -\sin \beta_i & \cos \beta_i \sin \gamma_i & \cos \beta_i \cos \gamma_i \end{bmatrix} \quad (109)$$

for  $i = 1, 2, 3$  and  $\alpha_i, \beta_i, \gamma_i$  are small angles. If  $\hat{e}_i$  are the unit vectors,  $\hat{n}$  and  $\hat{j}$  are given by

$$\hat{n}_i = \hat{e}_i R_i \quad (110)$$

5. We choose the magnetic fields scanning is done. We can do this in two ways as described in earlier section

type1 == 'A':  $B = B_1, B_2, B_3, \dots$  where  $B_i$  are given.

type2 == 'B':  $B = x_i B_{max}$  where  $x_i$  are the positive roots of even degree Legendre polynomial.

6. If we take  $n = 240$  and  $t_j = 2\pi j/n$  for  $0 \leq j < n$ , We will have  $\hat{n}_{i,j} = \hat{n}_i Rot(t_j)$  and  $\hat{j}_{i,j} = \hat{j}_i Rot(t_j)$ . Also we take temperature  $T_0$  and  $T_1$  and print the value of voltage  $V(\hat{n}_{i,j}, \hat{j}_{i,j}, \vec{B}_0, T)$  for  $i = 1, 2, 3$ ,  $0 \leq j < n$ , all  $B$  with the temperatures  $T_0$  and  $T_1$ .

Complete details can be found in the file [https://github.com/pritindra-bhowmick/Hall\\_Probes\\_3D\\_calibration\\_CERN/blob/main/generate\\_voltage.py](https://github.com/pritindra-bhowmick/Hall_Probes_3D_calibration_CERN/blob/main/generate_voltage.py)

## 5.2 The module that does it all

We have made a module to scan and give with two primary and a few basic functions to do our job. Once we have generated the data, there are two next steps: 1. Calculating parameters and 2. Building the model and reverting equation. They are done with two function `scan_3D` and `findB`. We will discuss the module in this section. This will not be a line by line explanation of the python code but it will give one the idea of where to look for for the details and math behind it.

### 5.2.1 Basic functions

There are 3 basic function used throughout the code

1. **Integrate(y,ba)**: This is the function for numerically integrating a function using the Simpson's 1/3 method as described in 4.1. Here **y** is the array of values of functions in the interval which are given by  $f(x_i)$  where  $x_i = x_0 + ih$ . **ba** =  $nh = b - a = x_n - x_0$ .
2. **lagrange\_even(x,y,xx)**: This is the function that takes arrays **x** =  $[x_0, x_1, x_2, \dots, x_n]$  and **y** =  $[y_0, y_1, y_2, \dots, y_n]$  and calculates the Lagrange interpolation polynomial given in 4.5.2 for even functions. Then it gives the interpolated value of function at **xx**, ie.,  $\mathbb{L}(\mathbf{xx})$
3. **getAngle(x)**: Gets the polar angle  $\phi$  and azimuthal angle  $\theta$  of the vector **x** in spherical coordinates.

### 5.2.2 scan\_3D

In this section, we will discuss the working of **scan\_3D** function. The function takes input in the form of a file that contains hall voltages and other parameters. Each part of the function is labelled with a number and a title. We will give descriptions of each point.

1. Scanning voltages generated **generate\_voltage.py** or calibration machine along with other parameters.
2. Opening output files to write down calculated parameters.
3. making angle and spherical harmonic arrays. We create all the spherical harmonics arrays in the beginning so that they are in the memory whenever we may need them. It decreases the time complexity by a lot by directly accessing them from memory. **Ylmarray(1,m)** function returns arrays with  $Y_{lm}$  values for the  $n = 240$  points.
4. Treating mixing of spherical harmonics as described in sections 3.1.1, 4.1 and 4.2.
5. Defining functions that give the values of spherical harmonics coefficient  $c_{lm}$ . We have 3 functions which takes arrays as inputs and gives out the coefficients as output. They are based on sections 3.1,4.1,4.2.They are **SphericalHarmonicCoeff**, **SphericalHarmonicCoeff00** and **SphericalHarmonicCoeffmag**.
6. Treating non-orthogonality as discussed in sections 3.2 and 4.3.
7. Linear fit for temperature dependence as discussed in sections 3.5 and 4.4.
8. Calculating  $\vec{r}_l$  as discussed in section 4.5.1.
9. Scaling coefficients with magnetic field strength as discussed in sections 3.4 and 4.5.

### 5.2.3 FindB

In this section, we will discuss the working of **findB** function. The function takes input in the form of a file that contains parameters, temperature and hall voltages from 3 hall probes. The 1st part scans all the parameters from the file. The 2nd part builds the model based on these parameters and the 3rd part solves non-linear equations to give



the magnetic field corresponding to the the given hall voltages and temperature. The mathematics and analysis behind this function can be found in sections 3.6, 4.6 and 4.7.

Complete module can be found at [https://github.com/pritindra-bhowmick/Hall\\_Probes\\_3D\\_calibration\\_CERN/blob/main/HallCalibration.py](https://github.com/pritindra-bhowmick/Hall_Probes_3D_calibration_CERN/blob/main/HallCalibration.py)

## 6 Results